CHEMISTRY
A EUROPEAN JOURNAL

DOI: 10.1002/chem.200801128

# π-Bonding in Complexes of Benzannulated Biscarbenes, -germylenes, and -stannylenes: An Experimental and Theoretical Study

**F. Ekkehardt Hahn,*[a] Alexander V. Zabula,[a] Tania Pape,[a] Alexander Hepp,[a] Ralf Tonner,[b, c] Robin Haunschild,[b] and Gernot Frenking[b]**

**Abstract:** Benzannulated bisstannylenes, exhibiting a $CH_2C(CH_3)_2CH_2$ linking unit and $CH_2tBu$ (**1**) or $CH_2CH_2CH_2NMe_2$ (**2**) *N*-substituents, and their molybdenum tetacarbonyl complexes **3** and **4** have been prepared. The complexes **3** and **4** exhibit remarkably short Mo–E bond lengths compared to the related biscarbene and bisgermylene complexes. The experimentally determined bonding parameters of the molybdenum bisstannylene complexes are discussed based on DFT calculations.

**Keywords:** carbene analogues · coordination modes · stannylenes · tin

## Introduction

The coordination chemistry of the heavier analogues of N-heterocyclic carbenes (NHCs)[1] has attracted considerable attention in the last decade due to their potential role as ligands for transition metals.[2] NHC ligands are usually considered strong σ donors and weak π acceptors (Scheme 1).[3] A similar bonding situation has been suggested for the heavier analogues—silylenes, germylenes, and stannylenes.[4] However, recent theoretical studies suggested that NHC ligands may also serve as π donors when they are bound to an electron-deficient metal atom.[5] This might in principle also be found for the heavier analogues of NHCs, but there have been only few corresponding reports in the literature so far. In this paper we report experimental and theoretical studies that shed new light on the bonding situation in complexes of N-heterocyclic carbenes, germylenes, and stannylenes.

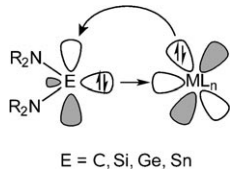


Scheme 1. Proposed bonding in complexes of diaminocarbenes and their heavier analogues.

We have described the preparation and coordination chemistry with different transition metals of bridged benzannulated biscarbenes **A**[6] and bisgermylenes **B** (Scheme 2).[7]

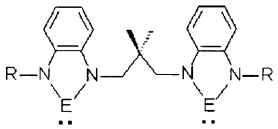


Scheme 2. Bridged benzannulated N-heterocyclic biscarbenes, bisgermylenes and bisstannylenes.

We became interested in the corresponding bisstannylenes with alkyl or Lewis basic functional groups **C** (Scheme 2). Here we describe the preparation and properties of bisstannylenes of type **C** and compare their coordination chemistry with $Mo^0$ to that of the biscarbene and bisgermylene analogues **A** and **B**.

## Results and Discussion

While some bis(diorganostannylene) ligands are known,[8] only few examples for potentially chelating benzannulated

[a] Prof. Dr. F. E. Hahn, Dr. A. V. Zabula, T. Pape, Dr. A. Hepp
Institut für Anorganische und Analytische Chemie
Westfälische Wilhelms-Universität Münster
Corrensstrasse 36, 48149 Münster (Germany)
Fax: (+49) 251-833-3108
E-mail: fehahn@uni-muenster.de

[b] Dr. R. Tonner, Dr. R. Haunschild, Prof. Dr. G. Frenking
Fachbereich Chemie, Philipps-Universität Marburg
Hans Meerwein Strasse, 35032 Marburg (Germany)

[c] Dr. R. Tonner
New address:
Center for Theoretical Chemistry and Physics
New Zealand Institute for Advanced Study
Massey University, Auckland (New Zealand)

Supporting information for this article is available on the WWW under http://dx.doi.org/10.1002/chem.200801128.

bisstannylenes have been reported so far[9] next to some monodentate benzannulated N-heterocyclic stannylenes.[10] We have prepared the bisstannylenes with a $CH_2C(CH_3)_2CH_2$ bridging group and *N*-neopentyl (**1**) or *N*-3-dimethylaminopropyl substituents (**2**) by the transamination reaction between the corresponding tetraamines[7a] and $[Sn\{N(SiMe_3)_2\}_2]$[11] (Scheme 3). The bisstannylene **2** is a

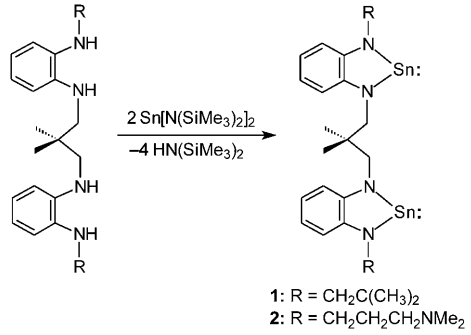


Scheme 3. Preparation of bisstannylenes **1** and **2**.

yellow solid that is moderately soluble in aromatic hydrocarbons and THF, while **1** is insoluble in toluene. Both **1** and **2** are sensitive to moisture and air.

The molecular structure of the *N*-donor functionalized bisstannylene **2** was determined by X-ray diffraction (Figure 1). Both tin atoms in **2** are stabilized by intramolecu-

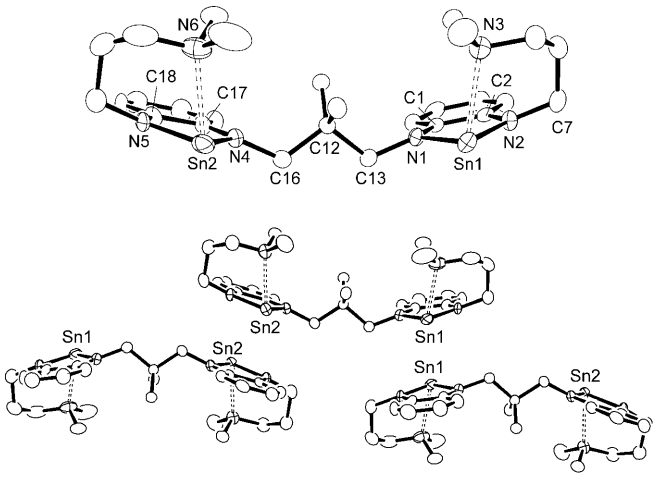


Figure 1. Molecular structure of bisstannylene **2** (top) and intermolecular interaction of three bisstannylene molecules (bottom). Selected bond lengths [Å] and angles [°]: Sn1–N1 2.090(3), Sn1–N2 2.063(3), Sn1–N3 2.561(4), Sn2–N4 2.082(4), Sn2–N5 2.067(4), Sn2–N6 2.530(4); N1-Sn1-N2 78.56(13), N1-Sn1-N3 100.10(12), N2-Sn1-N3 78.57(12), N4-Sn2-N5 78.19(15), N4-Sn2-N6 101.50(13), N5-Sn2-N6 79.81(14).

lar Sn–$NMe_2$ donor–acceptor coordination with Sn1–N3 and Sn2–N6 bond lengths measuring 2.561(4) and 2.530(4) Å, respectively. These values like the other bond lengths and angles found for **2** are in good agreement with equivalent parameters reported for a series of monodentate benzannulated N-heterocyclic stannylenes.[10]

In addition to the intramolecular stabilization an intermolecular interaction of the empty p orbital at the tin atoms with the π system of the benzene ring of an anti-parallel-oriented adjacent molecule was observed for **2**. This interaction leads to a polymeric arrangement of the bisstannylene molecules in the crystal lattice. The distances between the tin atoms and the center of the benzene ring of neighboring molecules measure 3.338 and 3.807 Å. A similar interaction has been observed previously for *N*,*N*′-di(neopentyl)benzimidazolin-2-stannylene[12a] and -plumbylene.[12b]

The $^{119}Sn$ NMR spectrum of bisstannylene **2** does not show a dependence of the chemical shift ($\delta = 95.0$ ppm in $[D_8]$THF, $\delta = 95.6$ ppm in $[D_8]$toluene) from the solvent in contrast to the observation made for the coordinatively unsaturated bisstannylene **1** ($\delta = 178.0$ ppm in $[D_8]$THF, $\delta = 200.9$ ppm in $[D_8]$THF/standard toluene). Apparently, the intramolecular Sn–$NMe_2$ coordination in **2** is maintained in both solvents. The *N*-alkyl-substituted, coordinatively unsaturated bisstannylene **1** on the other hand, experiences THF coordination in this solvent with the concurrent observation of a high-field shift of the $^{119}Sn$ resonance.[10]

The molybdenum complexes **3** and **4** of the bisstannylenes **1** and **2** have been synthesized by employing a methodology we have developed previously for the preparation of molybdenum complexes with bisgermylenes (Scheme 4).[7] Com-

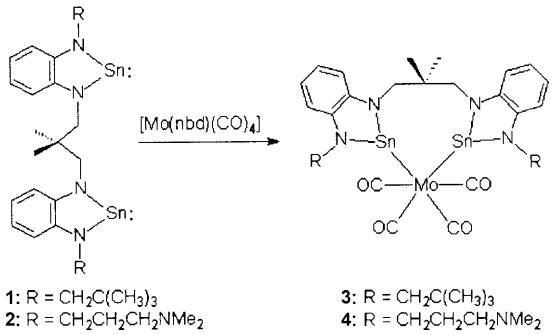


Scheme 4. Preparation of complexes **3** and **4**.

plexes **3** and **4** are air-sensitive red or orange solids, which can be recrystallized from toluene or THF. The $^{119}Sn$ NMR spectra of **3** show a strong dependence of the chemical shift from the solvent ($\delta = 432.0$ ppm in $[D_8]$toluene, $\delta = 349.5$ ppm in $[D_8]$THF) indicative of THF coordination to the tin center in this solvent. The upfield shift of the $^{119}Sn$ resonance for **4** ($\delta = 299.1$ ppm in $[D_8]$THF) on the other hand demonstrates intramolecular Sn–$NMe_2$ coordination.

An X-ray diffraction analysis with crystals of **3** (Figure 2) shows the molecular structure of this complex to be related to the analogous biscarbene (ligand **A**, **5**)[6b] and bisgermylene (ligand **B**, **6**)[7a] complexes. The Mo–Sn distances (2.6850(3) and 2.6736(4) Å) are elongated by about 0.36 Å compared to the Mo–C bond lengths in biscarbene complex **5**[6b] and are about 0.15 Å longer than in bisgermylene com-

  

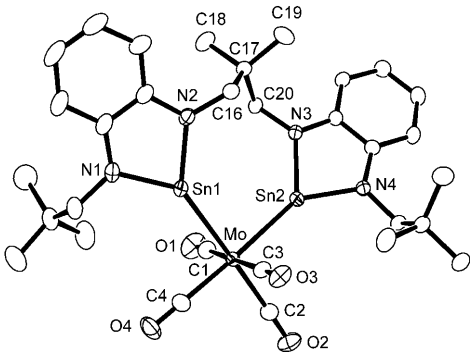


Figure 2. Molecular structure of complex **3**. Selected bond lengths [Å] and angles [°]: Mo–Sn1 2.6850(3), Mo–Sn2 2.6736(4), Mo–C1 2.053(2), Mo–C2 2.004(2), Mo–C3 2.035(2), Mo–C4 1.991(2), Sn1–N1 2.024(2), Sn1–N2 2.034(2), Sn2–N3 2.040(2), Sn2–N4 2.018(2), C1–O1 1.139(3), C2–O2 1.139(3), C3–O3 1.142(3), C4–O4 1.148(3); Sn1-Mo-Sn2 89.734(12), N1-Sn1-N2 81.48(7), N3-Sn2-N4 81.25(7).

plex **6**[7a] (Table 1), reflecting the increasing atomic radius C < Ge < Sn. The differences in the intracyclic E–N distances are much more pronounced for the transitions E = C (**5**)→E = Ge (**6**) (0.45 Å) and E = Ge (**6**)→E = Sn (**3**) (0.20 Å).

Table 1 shows that the Mo–$CO_{trans}$ distances (2.004(2) and 1.991(2) Å) are significantly shorter than the Mo–$CO_{cis}$ bond lengths (2.035(2) and 2.053(2) Å) and are similar to those found for the bisgermylene complex **6**. The difference between the Mo–$CO_{trans}$ and Mo–$CO_{cis}$ bond lengths in **3** (≈0.04 Å) is smaller than in the analogous biscarbene complex **6** (≈0.07 Å).

While M–CO bond lengths are not a good indicator of the electronic situation in carbonyl complexes, the wavenumbers of the $\nu$(CO) stretching modes are. The vibrational frequencies for the $\nu$(CO) stretching modes in **3** are similar to those observed for the analogous bisgermylene complex **6**. They are significantly higher than the $\nu$(CO) frequencies found for the biscarbene complex **5** (Table 1). These findings indicate that the bisstannylenes and bisgermylenes are either better π acceptors or weaker σ/π donors than the biscarbene. Note that the $\nu$(CO) frequencies in **3** and **6** are similar to those observed for alkylphosphite complexes of type *cis*-[Mo{PR(OR′)$_2$}$_2$(CO)$_4$],[13] which is in good agreement with theoretical predictions for the influence of diaminogermylenes on transition metal complex fragments.[14]

The molecular parameters of bisstannylene complex **4** (Figure 3) with the donor-functionalized N-substituents are

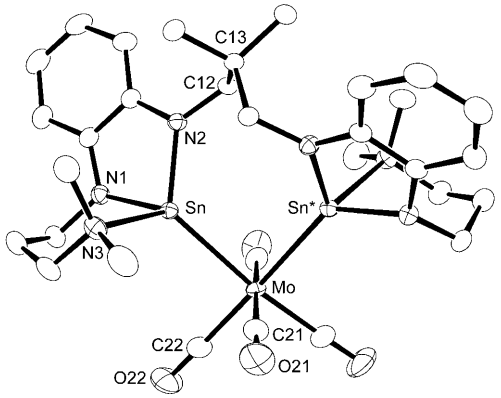


Figure 3. . Molecular structure of the complex **4**. Selected bond lengths [Å] and angles [°]: Mo–Sn 2.7046(6), Mo–C21 2.026(2), Mo–C22 1.979(3), Sn–N1 2.033(2), Sn–N2 2.059(2), Sn–N3 2.390(2); Sn-Mo-Sn* 86.87(2), N1-Sn-N2 80.49(7), N1-Sn-N3 84.67(7), N2-Sn-N3 106.33(7).

different from those found for **3** (Figure 2, Table 2). As already observed for the free bisstannylene **2** the $NMe_2$ groups in **4** are intramolecularly coordinated to the tin

Table 2. Bond lengths [Å], angles [°] and $\nu$(CO) [cm$^{-1}$] for stretching modes in complexes **3** and **4** and bisstannylene **2**.

| | **3** | **4** | **2** |
|---|---|---|---|
| $d$(Sn–Mo) | 2.6736(4), 2.6850(3) | 2.7046(6) | – |
| $d$(Sn–$N_{ring}$) | 2.018(2)–2.040(2) | 2.033(2), 2.059(2) | 2.063(3)–2.090(3) |
| $d$(Sn–$NMe_2$) | – | 2.390(2) | 2.530(4), 2.561(4) |
| $d$(Mo–$C_{cis}$) | 2.035(2), 2.053(2) | 2.026(2) | – |
| $d$(Mo–$C_{trans}$) | 1.991(2), 2.004(2) | 1.979(3) | – |
| $\nu$(CO), $A_1$ | 1947 | 1928 | |
| $\nu$(CO), $A_1$ | 2038 | 2008 | |

atoms. However, the Sn–$NMe_2$ distances in **4** (2.390(2) Å) are significantly shorter than in the free bisstannylene **2** (2.561(4) and 2.530(4) Å). At the same time the Mo–Sn bonds in **4** (2.7046(6) Å) are elongated compared to those found in complex **3** (2.6850(3) and 2.6736(4) Å).

The elongation of the Mo–Sn bonds in **4** relative to **3** is best explained by a less effective Mo(d)→Sn(p) π backbonding owing to electron donation of the $NMe_2$ group into the formally empty p orbital at the tin atom. Coordination of the tin atoms to molybdenum enhances the Lewis acidity of the p orbital at tin and thus leads to a

Table 1. Bond lengths [Å], angles [°] and $\nu$(CO) [cm$^{-1}$] for the stretching modes in complexes **3**, **5** and **6**.

| | **5**[6b] (E=$C_{carbene}$) | **6**[7a] (E=Ge) | **3** (E=Sn) |
|---|---|---|---|
| $d$(Mo–E) | 2.324(3) | 2.5189(6), 2.5204(6) | 2.6736(4), 2.6850(3) |
| $d$(E–N) | 1.367(4), 1.385(4) | 1.823(3)–1.827(3) | 2.018(2)–2.040(2) |
| $d$(Mo–$C_{cis}$) | 2.035(3) | 2.030(5), 2.047(4) | 2.035(2), 2.053(2) |
| $d$(Mo–$C_{trans}$) | 1.963(3) | 1.997(4), 1.998(4) | 1.991(2), 2.004(2) |
| $\nu$(CO), $A_1$ | 1889[a] | 1942[a] | 1947[b] |
| $\nu$(CO), $A_1$ | 2002[a] | 2031[a] | 2038[b] |
| $\nu$(CO), $B_1$ | 1857[a] | 1929[a] | 1929[b] |
| $\nu$(CO), $B_2$ | 1799[a] | 1908[a] | not observed |

[a] Infrared data. [b] Raman data ($\lambda_{exc}$ = 632.8 nm).

shorter Sn–$NMe_2$ bond in **4** compared to **2**. The shortening of the Sn–$NMe_2$ bonds and the elongation of Mo–Sn bonds in **4** compared to **3** indicate that Mo(d)→Sn(p) π backbonding is less pronounced in **4** than in **3**.

To analyze the Mo–Sn bonds in **3** we carried out DFT calculations at the BP86/TZ2P level[15] of the model compounds **3M** shown in Table 3 with E = C, Ge, Sn. The nature

Table 3. EDA (BP86/TZ2P) results for complexes of type **3M**.[a]

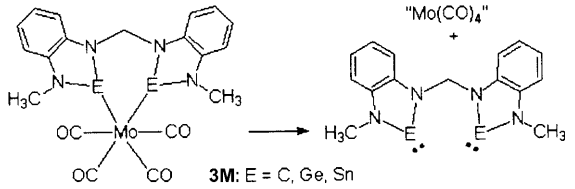


| | E = C | E = Ge | E = Sn |
|---|---|---|---|
| $\Delta E_{int}$ | −101.4 | −62.7 | −50.2 |
| $\Delta E_{Pauli}$ | 175.7 | 128.5 | 100.5 |
| $\Delta E_{elstat}$ | −175.2 (63.2 %) | −100.7 (52.7 %) | −74.6 (49.5 %) |
| $\Delta E_{orb}$ | −101.9 (36.8 %) | −90.5 (47.3 %) | −76.1 (50.5 %) |
| $\Delta E_{\sigma}$ | −75.9 (74.4 %) | −71.1 (78.6 %) | −62.1 (81.6 %) |
| $\Delta E_{\pi}$ | −26.1 (25.6 %) | −19.4 (21.4 %) | −14.0 (18.4 %) |
| $\Delta E_{prep}$ | 24.0 | 16.7 | 15.9 |
| $\Delta E\ (=-D_e)$ | −77.4 | −46.1 | −34.3 |
| $d$(Mo–E) | 2.232 | 2.530 | 2.733 |
| exptl value | 2.324(3) | 2.5204(6) | 2.6850(3) |
| | | 2.5189(5) | 2.6736(4) |

[a] All structures have been optimized under $C_{2v}$ symmetry constraints. Energy values are given in kcal mol$^{-1}$, interatomic distances in Å.

of the Mo–E interactions was then investigated with the energy decomposition analysis (EDA),[16] which has previously been used for a variety of transition-metal complexes.[17]

The DFT calculations predict that the Mo–E bond dissociation energies $D_e$ of **3M** decrease in the order C (77.4 kcal mol$^{-1}$) > Ge (46.1 kcal mol$^{-1}$) > Sn (34.3 kcal mol$^{-1}$). The EDA values suggest that the covalent character of the Mo–E bond given by the percentage values of the orbital term $\Delta E_{orb}$ increase from carbon (36.8 %) to tin (50.5 %). The contribution of the σ bonding is clearly larger than the π bonding, but the latter is not negligible. Note that the contribution of the π-orbital interactions to the $\Delta E_{orb}$ term decreases from 25.6 % in the carbene complex to 18.4 % in the stannylene complex.

The comparison of the theoretical and experimental bond lengths shows that the observed Mo–Sn distance in **3** (≈2.68 Å) is somewhat shorter than the calculated value for **3Sn** (2.733 Å), while the calculated value for the germylene species **3Ge** (2.530 Å) agrees quite well with the experimental value (≈2.52 Å), and the theoretical value for the carbene complex **3C** (2.232 Å) is even shorter than the experimental result (≈2.32 Å). This may be explained with the finding that bond lengths of donor–acceptor bonds tend to become shorter in the solid state than in the gas phase, and that the shortening increases for weaker bonds.[18]

We also calculated complexes between $NMe_3$ and benzannulated N-heterocyclic carbenes, germylenes, and stannylenes in order to study the strength of the N→E donor–acceptor interactions. The geometry optimization of the carbene did not yield a stable complex, while the germylene ($D_e$ = 1.6 kcal mol$^{-1}$) and stannylene ($D_e$ = 3.3 kcal mol$^{-1}$) species gave weakly bonded adducts. The calculated N–Sn distance (2.799 Å) is longer than the experimental value in **2** (2.530(4)–2.561(4) Å), which again can be explained with the bond-shortening solid-state effect on the weak interactions.[18]

The calculated π bonding contribution to the Mo–ligand interactions $\Delta E_{\pi}$ indicates the trend **3C** > **3Ge** > **3Sn**. How can this be reconciled with the trend of the CO stretching frequencies? A first hint comes from a comparison of the vibrational frequencies of the carbene, germylene, and stannylene complexes with the parent system [$Mo(CO)_6$]. The wavenumbers for the IR-active CO stretching modes of [$Mo(CO)_6$] are 2121.6 cm$^{-1}$ ($A_{1g}$) and 2026.6 cm$^{-1}$ ($E_g$), while the Raman data are 2119.7 cm$^{-1}$ ($A_{1g}$) and 2025.2 cm$^{-1}$ ($E_g$).[19] Comparing these values with the wavenumbers given in Table 1 could lead to the conclusion that the $E^{II}$ ligands in **3**, **5**, and **6** are π donors rather than π acceptors. This proposition would be in conflict, however, with the above explanation of the shortening of the Sn–$NMe_2$ bond and the elongation of the Mo–Sn bond in **4** compared to **3**. A further analysis of the model compounds [$(CO)_5$Mo–$EN_2C_2H_4$] (E = C, Ge, Sn) in which $EN_2C_2H_4$ is a N-heterocyclic carbene, germylene, or stannylene explains the trend of the CO stretching modes.

The Mo→CO π backdonation has two components, one is perpendicular to the $EN_2C_2H_4$ plane ($\pi_{\perp}$), while the other one is in the plane ($\pi_{\parallel}$).[20] The $\Delta E_{\pi}$ values in Table 3 give only the $\pi_{\perp}$ contribution of the Group 14 ligands to the bonding interactions, because the molecules have only $C_s$ symmetry. A charge analysis of [$(CO)_5$Mo–$EN_2C_2H_4$], which has $C_{2v}$ symmetry, shows that the $EN_2C_2H_4$ ligand is a very weak $\pi_{\perp}$ acceptor with $\Delta q(\pi_{\perp})$ = −0.064 e (C), −0.075 e (Ge), and −0.065 e (Sn) and a weak $\pi_{\parallel}$ acceptor with $\Delta q(\pi_{\parallel})$ = −0.043 e (C), −0.046 e (Ge), and −0.054 e (Sn). However, the CO ligand *trans* to $EN_2C_2H_4$ also receives π charge in the complex! The calculated $\Delta q(\pi)$ values of $CO_{trans}$ in [$(CO)_5$Mo–$EN_2C_2H_4$] are −0.084 e (C), −0.078 e (Ge), and −0.091 e (Sn). The largest changes and highest absolute values are found for the [$(CO)_5$Mo←$EN_2C_2H_4$] σ donation. The calculated values are $\Delta q(\sigma)$ = 0.593 e (C), 0.503 e (Ge), and 0.247 e (Sn). Thus, the very strong [$(CO)_5$Mo←$EN_2C_2H_4$] σ donation makes the molybdenum atom a stronger π donor, which yields π backdonation towards both ligands [(OC)←Mo→$EN_2C_2H_4$]. The charge analysis suggests that the trend of the CO stretching modes **3C** < **3Ge** < **3Sn** comes from the [$(CO)_5$Mo←$EN_2C_2H_4$] σ donation and not from π bonding! Note that the stretching frequency and force constant of CO is much higher in protonated $HCO^+$, in which CO is bound to a strong σ acceptor.[21] The shift of the CO stretching frequencies toward lower wave numbers **3C** < **3Ge** < **3Sn** is in agreement with

  

the significant change of the $(CO)_5Mo{\leftarrow}EN_2C_2H_4$ σ donation.[22]

## Conclusion

Benzannulated bisstannylenes and their complexes have been prepared and investigated. It was found that bisstannylene and bisgermylene ligands act not only as a σ donor and π acceptor, but also function as π donors.

## Experimental Section

For details of the reaction conditions see references [7a,910].

**Data for 1**: Yield 90%; bright yellow solid; $^1$H NMR (400 MHz, [D$_8$]THF): $\delta = 6.81$ (m, 4H; Ar-H), 6.51 (m, 4H; Ar-H), 4.14 (s, 4H; $CH_2C(CH_3)_2CH_2$), 3.89 (s, 4H; $CH_2C(CH_3)_3$), 1.17 (s, 6H; $C(CH_3)_2$), 0.98 ppm (s, 18H; $C(CH_3)_3$); $^{13}$C NMR (100.6, [D$_8$]THF): $\delta = 147.6$, 147.5 (Ar-C$_{ipso}$), 116.2, 116.0 (Ar-C$_{meta}$), 110.2, 110.0 (Ar-C$_{ortho}$), 58.7 ($CH_2C(CH_3)_3$), 57.3 ($CH_2C(CH_3)_2CH_2$), 39.2 ($C(CH_3)_2$), 33.9 ($C(CH_3)_3$), 29.1 ($C(CH_3)_3$), 27.0 ppm ($C(CH_3)_2$); $^{119}$Sn NMR (149.2 MHz, [D$_8$]THF): $\delta =$ 178.0 ppm; $^{119}$Sn NMR (149.2 MHz, [D$_8$]THF + toluene (v:v = 1:1)): $\delta =$ 200.9 ppm; MS (70 eV): *m/z* (%): 658 (31) $[M]^+$, 601 (33) $[M-t\mathrm{Bu}]^+$, 540 (100) $[M-\mathrm{Sn}]^+$, 483 (55) $[M-t\mathrm{Bu}-\mathrm{Sn}]^+$; elemental analysis calcd (%) for $C_{27}H_{40}N_4Sn_2$: C 49.28, H 6.13, N 8.51; found: C 49.24, H 6.45, N, 8.26.

**Data for 2**: Yield 60%; recrystallized from toluene as yellow crystals; $^1$H NMR (400 MHz, [D$_8$]toluene): $\delta = 6.96$–6.94 (m, 2H; Ar-H), 6.91–6.88 (m, 4H; Ar-H), 6.77–6.74 (m, 2H; Ar-H), 3.98 (s, 4H; $NCH_2C(CH_3)_2CH_2$), 3.80 (t, $J = 5.3$ Hz, 4H; $NCH_2CH_2CH_2$), 1.98 (t, $J = 5.4$ Hz, 4H; $NCH_2CH_2CH_2$), 1.57 (s, 12H; $CH_2N(CH_3)_2$), 1.45 (m, 4H; $CH_2CH_2N(CH_3)_2$), 1.18 ppm (s, 6H; $CH_2C(CH_3)_2CH_2$); $^{13}$C NMR (100.6 MHz, [D$_8$]toluene): $\delta = 149.1$, 146.2 (Ar-C$_{ipso}$), 116.5, 116.1 (Ar-C$_{meta}$), 110.5, 108.8 (Ar-C$_{ortho}$), 60.3, 58.2 ($NCH_2$), 46.1 ($CH_2CH_2N(CH_3)_2$), 45.1 ($CH_2N(CH_3)_2$), 39.1 ($CH_2C(CH_3)_2CH_2$), 27.0 ($CH_2CH_2N(CH_3)_2$), 25.0 ppm ($CH_2C(CH_3)_2CH_2$); $^{119}$Sn NMR (149.2 MHz, [D$_8$]toluene): $\delta =$ 95.6 ppm; $^{119}$Sn NMR (149.2 MHz, [D$_8$]THF): $\delta = 95.0$ ppm; MS (70 eV): *m/z* (%): 688 (5) $[M]^+$, 570 (100) $[M-\mathrm{Sn}]^+$.

**Data for 3**: Yield 83%; recrystallized from toluene as red crystals; $^1$H NMR (400 MHz, [D$_8$]THF): $\delta = 6.86$–6.84 (m, 4H; Ar-H), 6.57–6.52 (m, 4H; Ar-H), 3.87 (s, 4H; $NCH_2$), 3.83 (s, 4H; $NCH_2$), 1.08 (s, 18H; $C(CH_3)_3$), 1.01 ppm (s, 6H; $CH_2C(CH_3)_2CH_2$); $^{13}$C NMR (100.6 MHz, [D$_8$]THF): $\delta = 217.6$ (CO$_{trans}$), 209.5 (CO$_{cis}$), 147.0, 146.9 (Ar-C$_{ipso}$), 116.4, 115.9 (Ar-C$_{meta}$), 110.7, 109.8 (Ar-C$_{ortho}$), 59.1 ($NCH_2C(CH_3)_3$), 51.5 ($CH_2C(CH_3)_2CH_2$), 41.4 ($CH_2C(CH_3)_2CH_2$), 35.2 ($CH_2C(CH_3)_3$), 29.3 ($CH_2C(CH_3)_3$), 25.8 ppm ($CH_2C(CH_3)_2CH_2$); $^{119}$Sn NMR (149.2 MHz, [D$_8$]toluene): $\delta = 432.0$ ppm ($^2J(^{119}\mathrm{Sn},^{117}\mathrm{Sn}) = 1470$ Hz); $^{119}$Sn NMR (149.2 MHz, [D$_8$]THF): $\delta = 349.5$ ppm; Raman spectrum (pure substrate): $\tilde{\nu}(\mathrm{CO}) = 2038$ (vs, A$_1$), 1947 (s, A$_1$), 1929 cm$^{-1}$ (s, B$_1$).

**Data for 4**: Yield: 90%; recrystallized from THF as orange crystals; $^1$H NMR (400 MHz, [D$_8$]THF): $\delta = 6.73$ (d, $J = 7.7$ Hz, 2H; Ar-H), 6.65 (d, $J = 7.7$ Hz, 2H; Ar-H), 6.52 (t, $J = 7.5$ Hz, 2H; Ar-H), 6.46 (t, $J = 7.6$ Hz, 2H; Ar-H), 4.10 (t, $J = 5.0$ Hz, 4H; $NCH_2CH_2CH_2$), 3.70 (s, 4H; $CH_2C(CH_3)_2CH_2$), 2.88 (t, $J = 5.2$ Hz, 4H; $CH_2CH_2N(CH_3)_2$), 2.12 (s, 12H; $CH_2N(CH_3)_2$), 1.90 (m, 4H; $NCH_2CH_2CH_2$), 1.12 ppm (s, 6H; $CH_2C(CH_3)_2CH_2$); $^{13}$C NMR (100.6 MHz, [D$_8$]THF): $\delta = 218.9$ (CO$_{trans}$), 211.0 (CO$_{cis}$), 148.6, 146.3 (Ar-C$_{ipso}$), 117.0, 115.7 (Ar-C$_{meta}$), 111.4, 108.0 (Ar-C$_{ortho}$), 62.8, 52.6 ($NCH_2$), 46.9 ($CH_2CH_2N(CH_3)_2$), 46.7 ($CH_2N(CH_3)_2$), 40.1 ($CH_2C(CH_3)_2CH_2$), 25.4 ($CH_2CH_2CH_2N(CH_3)_2$), 24.5 ppm ($CH_2C(CH_3)_2CH_2$); $^{119}$Sn NMR (149.2 MHz, [D$_8$]THF): $\delta = 299.1$ ppm.

**X-ray structure determinations**

*Data for* ***2***: $C_{27}H_{42}N_6Sn_2$, $M_r = 688.05$, yellow crystal, $0.11 \times 0.06 \times 0.03$ mm$^3$, $a = 9.9259(2)$, $b = 11.632(2)$, $c = 13.394(3)$ Å, $\alpha = 102.759(4)$, $\beta = 94.218(4)$, $\gamma = 105.928(4)°$, $V = 1435.4(5)$ Å$^3$, $\rho_{calcd} = 1.592$ g cm$^{-3}$, $\mu = 1.766$ mm$^{-1}$, 14228 measured intensities ($3.2 \le 2\theta \le 55.0°$), $\lambda = 0.71073$ Å, $T = 153(2)$ K, semiempirical absorption correction (min/max transmission 0.8295/0.9489), 6560 independent intensities ($R_{int} = 0.0522$), 4641 observed intensities, triclinic, $P\bar{1}$, $Z = 2$, $R = 0.0443$, $wR = 0.0689$ for 4641 contributing reflections [$I \ge 2\sigma(I)$], refinement of 368 parameters against $|F^2|$ of all unique reflections with hydrogen atoms on calculated positions.

*Data for* ***3***: $C_{31}H_{40}N_4MoO_4Sn_2$, $M_r = 865.99$, red crystal, $0.41 \times 0.37 \times 0.21$ mm$^3$, $a = 10.892(2)$, $b = 19.450(3)$, $c = 15.846(2)$ Å, $\beta = 92.385(3)°$, $V = 3354.1(9)$ Å$^3$, $\rho_{calcd} = 1.715$ g cm$^{-3}$, $\mu = 1.885$ mm$^{-1}$, 37663 measured intensities ($3.3 \le 2\theta \le 60.0°$), $\lambda = 0.71073$ Å, $T = 153(2)$ K, semiempirical absorption correction (min/max transmission 0.5120/0.6929), 9710 independent intensities ($R_{int} = 0.0287$), 8973 observed intensities, monoclinic, $P2_1/n$, $Z = 4$, $R = 0.0267$, $wR = 0.0590$ for 8973 contributing reflections [$I \ge 2\sigma(I)$], refinement of 387 parameters against $|F^2|$ of all unique reflections with hydrogen atoms on calculated positions.

*Data for* ***4***·$C_7H_8$: $C_{38}H_{50}N_6MoO_4Sn_2$, $M_r = 988.17$, orange crystal, $0.18 \times 0.15 \times 0.10$ mm$^3$, $a = 21.271(6)$, $b = 15.277(4)$, $c = 15.298(4)$ Å, $\beta = 127.716(4)°$, $V = 3932(2)$ Å$^3$, $\rho_{calcd} = 1.715$ g cm$^{-3}$, $\mu = 1.668$ mm$^{-1}$, 22466 measured intensities ($3.6 \le 2\theta \le 60.2°$), $\lambda = 0.71073$ Å, $T = 153(2)$ K, semiempirical absorption correction (min/max transmission 0.7591/0.8547), 5726 independent intensities ($R_{int} = 0.0343$), 4954 observed intensities, monoclinic, $C2/c$, $Z = 4$, $R = 0.0271$, $wR = 0.0617$ for 4954 contributing reflections [$I \ge 2\sigma(I)$], refinement of 248 parameters against $|F^2|$ of all unique reflections with hydrogen atoms on calculated positions. The asymmetric unit contained $^1/_2$ a molecule of **4** that was bisected by a two-fold axis passing through atoms Mo and C13 and $^1/_2$ a molecule of disordered toluene.

CCDC 690688 (**2**), 690689 (**3**) and 690690 (**4**) contain the supplementary crystallographic data for this paper. These data can be obtained free of charge from The Cambridge Crystallographic Data Centre via www.ccdc.cam.ac.uk/data_request/cif.

## Acknowledgement

This work was supported by the Deutsche Forschungsgemeinschaft, the Fonds der Chemischen Industrie and the NRW Graduate School of Chemistry Münster. R.T. Thanks the German Academic Exchange service (DAAD) for financial support.

[1] a) F. E. Hahn, M. C. Jahnke, *Angew. Chem.* **2008**, *120*, 3166–3216; *Angew. Chem. Int. Ed.* **2008**, *47*, 3122–3172; b) O. Kaufhold, F. E. Hahn, *Angew. Chem.* **2008**, *120*, 4122–4126; *Angew. Chem. Int. Ed.* **2008**, *47*, 4057–4061.

[2] a) A. G. Avent, B. Gehrhus, P. B. Hitchcock, M. F. Lappert, H. Maciejewski, *J. Organomet. Chem.* **2003**, *686*, 321–331; b) B. Gehrhus, P. B. Hitchcock, M. F. Lappert, H. Maciejewski, *Organometallics* **1998**, *17*, 5599–5601; c) W. A. Herrmann, P. Härter, C. W. K. Gstöttmayr, F. Bielert, N. Seeboth, P. Sirsch, *J. Organomet. Chem.* **2002**, *649*, 141–146; d) T. A. Schmedake, M. Haaf, B. J. Paradise, A. J. Millevolte, D. R. Powell, R. West, *J. Organomet. Chem.* **2001**, *636*, 17–25; e) A. Zeller, F. Bielert, P. Haerter, W. A. Herrmann, T. Strassner, *J. Organomet. Chem.* **2005**, *690*, 3292–3299; f) A. Fürstner, H. Krause, C. W. Lehmann, *Chem. Commun.* **2001**, 2372–2373; g) E. Neumann, A. Pfaltz, *Organometallics* **2005**, *24*, 2008–2011; h) T. A. Schmedake, M. Haaf, B. J. Paradise, D. Powell, R. West, *Organometallics* **2000**, *19*, 3263–3265; i) W. A. Herrmann, M. Denk, J. Behrn, W. Scherer, F.-R. Klingan, H. Bock, B. Solouki, M. Wagner, *Angew. Chem.* **1992**, *104*, 1489–1492; *Angew. Chem. Int. Ed. Engl.* **1992**, *31*, 1485–1488; j) O. Kühl, P. Lönnecke, J. Heinicke, *Inorg. Chem.* **2003**, *42*, 2836–2838.

[3] a) R. Tonner, G. Heydenrych, G. Frenking, *Chem. Asian J.* **2007**, *2*, 1555–1567; b) S. Díez-González, S. P. Nolan, *Coord. Chem. Rev.* **2007**, *251*, 874–883; c) D. Nemcsok, K. Wichmann, G. Frenking, *Organometallics* **2004**, *23*, 3640–3646; d) D. A. Dixon, A. J. Arduengo, III, *J. Chem. Phys.* **1991**, *95*, 4180–4182; e) A. J. Arduengo III, H. V. Rasika Dias, R. L. Harlow, M. Kline, *J. Am. Chem. Soc.* **1992**, *114*,

  

5530–5534; f) C. Heinemann, T. Müller, Y. Apeloig, H. Schwarz, *J. Am. Chem. Soc.* **1996**, *118*, 2023–2038; g) C. Boehme, G. Frenking, *J. Am. Chem. Soc.* **1996**, *118*, 2039–2046.

[4] a) W. Petz, *Chem. Rev.* **1986**, *86*, 1019–1047; b) C. Boehme, G. Frenking, *Organometallics* **1998**, *17*, 5801–5809; c) D. S. McGuinness, B. F. Yates, K. J. Cavell, *Organometallics* **2002**, *21*, 5408–5414.

[5] a) N. M. Scott, R. Dorta, E. D. Stevens, A. Correa, L. Cavallo, S. P. Nolan, *J. Am. Chem. Soc.* **2005**, *127*, 3516–3526; b) H. Jacobsen, *J. Organomet. Chem.* **2005**, *690*, 6068–6078; c) H. Jacobsen, A. Correa, C. Costabile, L. Cavallo, *J. Organomet. Chem.* **2006**, *691*, 4350–4358.

[6] a) F. E. Hahn, M. Foth, *J. Organomet. Chem.* **1999**, *585*, 241–245; b) F. E. Hahn, L. Wittenbecher, D. Le Van, R. Fröhlich, *Angew. Chem.* **2000**, *112*, 551–554; *Angew. Chem. Int. Ed.* **2000**, *39*, 541–544; c) F. E. Hahn, T. von Fehren, L. Wittenbecher, R. Fröhlich, *Z. Naturforsch. B* **2004**, *59*, 541–543; d) F. E. Hahn, T. von Fehren, T. Lügger, *Inorg. Chim. Acta* **2005**, *358*, 4137–4144.

[7] a) A. V. Zabula, F. E. Hahn, T. Pape, A. Hepp, *Organometallics* **2007**, *26*, 1972–1980; b) F. E. Hahn, A. V. Zabula, T. Pape, A. Hepp, *Eur. J. Inorg. Chem.* **2007**, 2405–2408.

[8] M. Henn, M. Schürmann, B. Mahieu, P. Zanello, A. Cinquantini, K. Jurkschat, *J. Organomet. Chem.* **2006**, *691*, 1560–1572.

[9] a) A. V. Zabula, T. Pape, A. Hepp, F. M. Schappacher, U. Ch. Rodewald, R. Pöttgen, F. E. Hahn, *J. Am. Chem. Soc.* **2008**, *130*, 5648–5649; b) A. V. Zabula, T. Pape, A. Hepp, F. E. Hahn, *Organometallics* **2008**, *27*, 2756–2760; c) A. V. Zabula, T. Pape, A. Hepp, F. E. Hahn, *Dalton Trans.* **2008**, 5886–5890.

[10] F. E. Hahn, L. Wittenbecher, D. Le Van, A. V. Zabula, *Inorg. Chem.* **2007**, *46*, 7662–7667.

[11] D. H. Harris, M. F. Lappert, *J. Chem. Soc. Chem. Commun.* **1974**, 895–896.

[12] a) H. Braunschweig, B. Gehrhus, P. B. Hitchcock, M. F. Lappert, *Z. Anorg. Allg. Chem.* **1995**, *621*, 1922–1928; b) F. E. Hahn, D. Heitmann, T. Pape, *Eur. J. Inorg. Chem.* **2008**, 1039–1041.

[13] a) C. E. Jones, K. J. Coskran, *Inorg. Chem.* **1971**, *10*, 55–62; b) P. S. Bratermann, in *Metal Carbonyl Spectra*, Academic Press, London, New York, San Francisco, **1975**, pp. 217–220.

[14] O. Kühl, K. Lifson, W. Langel, *Eur. J. Org. Chem.* **2006**, 2336–2343.

[15] All calculations were carried out at the BP86 level: a) A. D. Becke, *Phys. Rev. A* **1988**, *38*, 3098–3100; b) J. P. Perdew, *Phys. Rev. B* **1986**, *33*, 8822–8824; the basis sets in this work have TZ2P quality: c) J. G. Snijders, P. Vernooijs, E. J. Baerends, *At. Data Nucl. Data Tables* **1981**, *26*, 483–509; all calculations were performed using the program package ADF: d) F. M. Bickelhaupt, E. J. Baerends in *Rev. Comput. Chem., Vol. 15* (Eds.: K. B. Lipkowitz, D. B. Boyd), Wiley-VCH, Weinheim, **2000**, p. 1; e) G. te Velde, F. M. Bickelhaupt, E. J. Baerends, S. J. A. van Gisbergen, C. Fonseca Guerra, J. G. Snijders, T. Ziegler, *J. Comput. Chem.* **2001**, *22*, 931–967; the full set of calculated geometries and energies is given as Supporting Information.

[16] T. Ziegler, A. Rauk, *Theor. Chim. Acta* **1977**, *46*, 1–10.

[17] a) G. Frenking, K. Wichmann, N. Fröhlich, C. Loschen, M. Lein, J. Frunzke, V. M. Rayón, *Coord. Chem. Rev.* **2003**, *238–239*, 55–82; b) M. Lein, G. Frenking in *Theory and Applications of Computational Chemistry: The First 40 Years* (Eds.: C. E. Dykstra, G. Frenking, K. S. Kim, G. E. Scuseria), Elsevier, Amsterdam, **2005**, pp. 291–372.

[18] V. Jonas, G. Frenking, M. T. Reetz, *J. Am. Chem. Soc.* **1994**, *116*, 8741–8753.

[19] M. R. Afiz, R. J. H. Clark, N. R. D'Urso, *J. Chem. Soc. Dalton Trans.* **1977**, 250–254.

[20] For a pictorial decription of the $\pi_{\perp}$ and $\pi_{\parallel}$ interactions in N-heterocyclic carbenes see reference [3a].

[21] E. Hirota, Y. Endo, *J. Mol. Spectrosc.* **1988**, *127*, 527–534.

[22] For a thorough discussion of the σ and π bonding in CO and the change through interactions with a σ acceptor see: A. J. Lupinetti, S. Fau, G. Frenking, S. H. Strauss, *J. Phys. Chem. A* **1997**, *101*, 9551–9559.

Received: June 10, 2008
Published online: October 17, 2008

  